The Role of Iron in the Formation of Porosity in Al-Si-Cu–Based Casting Alloys: Part III. A Microstructural Model

J.A. TAYLOR, G.B. SCHAFFER, and D.H. StJOHN

Iron has been shown to have a significant effect on the formation of porosity and shrinkage defects in Al-Si-Cu–based foundry alloys. This is not simply a direct consequence of the physical presence of the β-Al_5FeSi platelets in the microstructure, but is also due to the effect that these platelets have on the nucleation and growth of eutectic silicon. The alloy-dependent critical iron content determines when the β phase first solidifies and, hence, when it can participate in the silicon nucleation event. At critical iron contents, the β phase solidifies as the initial component of the ternary eutectic. However, at supercritical iron contents, the β phase is already well developed when ternary eutectic solidification begins, while, at subcritical iron contents, the β phase forms as a component of the ternary eutectic only after the binary Al-Si eutectic is well established. Each of these paths of microstructural evolution leads to different variations in microstructural permeability and, hence, interdendritic feedability and porosity formation. The actual porosity-forming response to these alloy-induced microstructural changes is influenced by the solidification conditions in the casting.

I. INTRODUCTION

VOLUMETRIC shrinkage occurs during the solidification of most alloys. In order to produce a casting free from slumping, contraction, and/or internal porosity, this shrinkage must be compensated by an unimpeded supply of feed liquid to solidifying regions. Anything which hinders this feeding will result in the formation of some type of shrinkage-related defect. Various researchers have proposed that the presence of β platelets within the interdendritic spaces of iron-containing Al-Si alloys causes physical blockages to interdendritic fluid flow and that these make feeding more difficult and defect formation easier.[1,2,3]

This "restricted feeding" theory cannot explain the experimental observations described in two companion articles.[4,5] In that work, iron is shown to play an important role in the development of porosity and shrinkage defects in unmodified, nongrain-refined hypoeutectic Al-Si alloys that also contain approximately 1 pct Cu and 0.5 pct Mg. The role of iron is manifest as a distinctive threefold effect that is also dependent on the silicon content of the alloy and which can be explained in terms of the solidification sequence.

At a critical iron content, solidification proceeds directly from primary dendrite formation to the formation of the ternary Al-Si-βAl_5FeSi eutectic. The minimum total porosity occurs at this iron level. As the iron content varies to either side of the critical value, the overall porosity increases. At supercritical iron contents, there is also an increase in the likelihood of localized, interconnected sponge porosity occurring. In the subcritical iron regime, a change in pore morphology is evident.

Microstructural examination has shown that the β phase is present at all iron levels from 0.1 to 1.0 pct. This suggests that it is not the β phase *per se* that is the cause of the detrimental porosity effects observed at high iron contents, as has been previously assumed.[1–3,6] Instead, it is more likely that an indirect relationship exists between the β phase and porosity formation.

The flow of fluid through a solidifying dendritic network has been compared to the flow of a fluid through a packed bed, using a relationship based on D'Arcy's law:[7]

$$Q = \frac{K \Delta P}{\mu L} \qquad [1]$$

where Q is the flow rate, ΔP is the pressure drop along a length L, μ is the viscosity, and K is the permeability of the bed, which, for a solidifying dendritic network, has been expressed as[7]

$$K = \frac{(f_L)^2}{8n\pi\tau^3} \qquad [2]$$

where f_L is the volume fraction of liquid, n is the number of channels per unit cross-sectional area, and τ is the "tortuosity" factor (a term used to account for the fact that the channels are neither straight nor smooth).

The parameters n and τ are typically assumed to be constant and, consequently, the permeability of a solidifying structure is assumed to be solely dependent on the diminishing volume fraction of liquid. However, various microstructural changes can lead to changes in permeability. For instance, in some alloys, both the number of channels per unit area and the tortuosity increase as the microstructure evolves. In such cases, it is reasonable to expect the permeability to drop to a value incapable of sustaining interdendritic flow earlier than if it depended solely upon the decreasing fraction of liquid. The microstructural evolution can, therefore, be important.

This article examines the mechanism by which iron affects the microstructural evolution of Al-Si-Cu alloys. In particular, we examine the relationship between the β phase and the nucleation of unmodified eutectic silicon and how this influences both the alloy feeding characteristics and the formation of porosity and shrinkage defects.

J.A. TAYLOR, formerly Doctoral Student, is Senior Research Fellow, CRC for Alloy and Solidification Technology (CAST), Department of Mining, Minerals and Materials Engineering, The University of Queensland. G.B. SCHAFFER, Reader, and D.H. StJOHN, Professor, are with CAST, Department of Mining, Minerals and Materials Engineering, The University of Queensland, Brisbane, QLD 4072, Australia.

Manuscript submitted March 27, 1998.

II. EXPERIMENTAL

Metallographic sections (polished to a colloidal silica finish and unetched) taken from several castings of the two experimental alloys[4,5] at various iron levels were examined, using optical microscopy, to study the relationship between the β phase and the eutectic silicon.

Selected metallographic samples were deep etched by immersion in a 1 pct aqueous solution of NaOH at 55 °C to 60 °C for a period of 10 minutes. This process removed the aluminum phase, leaving the iron-containing intermetallics and the eutectic silicon exposed. The deep-etched samples were then examined using a JEOL* JSM-6400F scanning electron microscope with a Link X-ray analytical facility. Several apparent nucleation events of unmodified eutectic silicon on the β platelets were studied in both experimental alloys. The etching depth was on the order of 10 μm. Since the large intermetallic platelet structures were typically >100 μm, the ratio of exposed surface to the submerged surface was low.

*JEOL is a trademark of Japan Electron Optics Ltd., Tokyo.

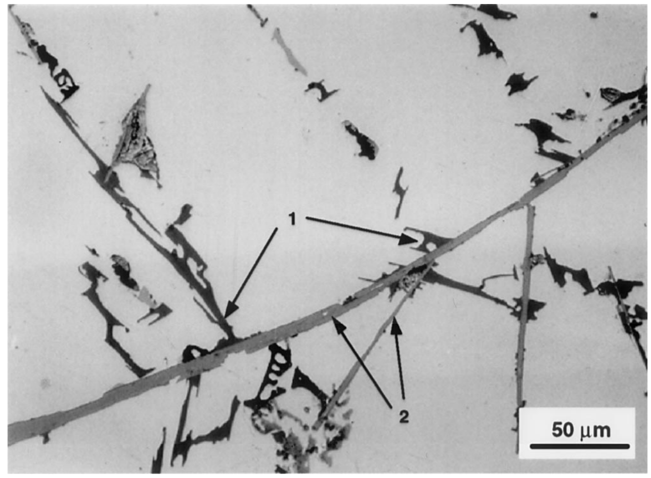

Fig. 1—Typical optical micrograph showing the eutectic silicon phase (medium gray, marked as 1) nucleating at several locations along the length of a large binary β-Al_5FeSi platelet (light gray, marked as 2) from the B7 segment of an AA309 alloy casting containing 0.55 pct Fe. The black phase is Mg_2Si.

III. RESULTS

Unmodified silicon eutectic was present in all samples (all alloy compositions/casting configurations/casting locations) and occurred as both fine acicular structures between the aluminium dendritic structure and as larger, isolated pools of coarse acicular structure. The most consistent observation regarding the formation of the unmodified eutectic silicon was the manner of its nucleation. In samples of both the AA309 alloy (approximately Al-5 pct Si-1 pct Cu-0.5 pct Mg) and the Al-10 pct silicon variant (approximately Al-10 pct Si-1 pct Cu-0.5 pct Mg), the β-Al_5FeSi platelets appeared to be the main nucleation sites for the eutectic silicon. (These β platelets also appeared to be the favored nucleation sites for other late-forming phases such as Mg_2Si and $CuAl_2$). Nucleation of silicon (both acicular and polygonal) occurred on both the large "binary" β platelets (formed as a component of the Al-βAl_5FeSi binary eutectic complex) and on the smaller "ternary" β platelets (formed as a component of the Al-Si-βAl_5FeSi ternary eutectic complex). Examples of these events in both alloy systems are shown in Figures 1 and 2.

The silicon was frequently observed to grow from multiple locations along a single β platelet and even, on occasion, to have completely engulfed small β platelets. The reverse situation of β platelets nucleating on or covering silicon was not observed. The iron-containing π-phase particles ($Al_8FeMg_3Si_6$) did not appear to participate in the nucleation of eutectic silicon. Scanning electron microscopy (SEM) of deep-etched samples also showed that eutectic silicon grows directly on the β phase. Figure 3 shows an example of an embryonic eutectic silicon cell nucleating on a β substrate. This silicon cell is not continuous with the background aluminum matrix, which implies that it nucleated on the β substrate and not on another source.

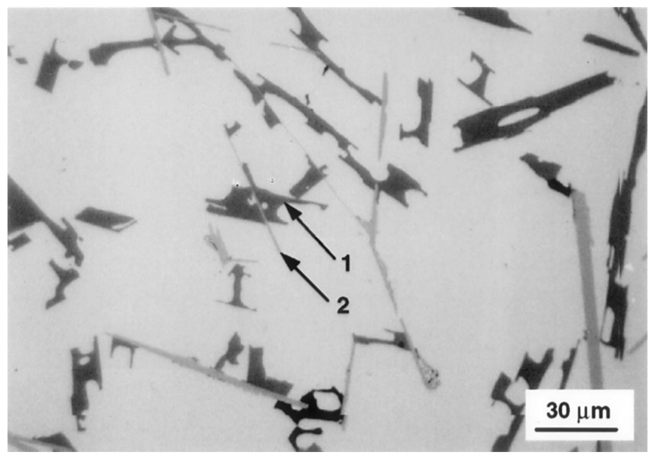

(*a*)

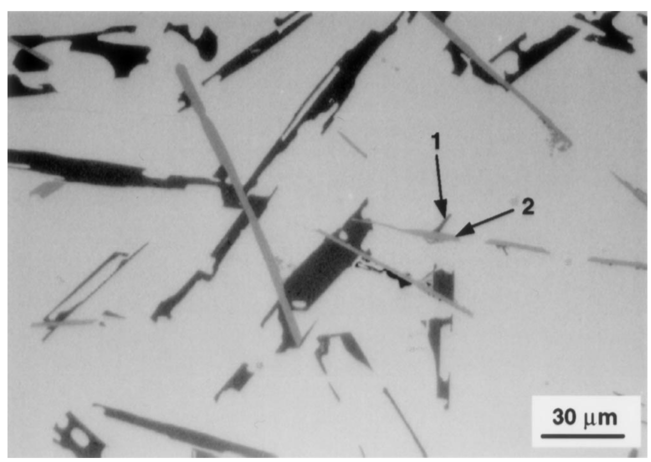

(*b*)

Fig. 2—Typical optical micrographs showing eutectic silicon phase (medium gray, marked as 1) nucleating on small-scale β-Al_5FeSi platelets (light gray colour, marked as 2), which may have formed as part of the Al-Si-Al_5FeSi ternary eutectic. These samples are from the C6 segments of 10 pct silicon alloy castings with iron contents of (*a*) 0.7 pct and (*b*)1.00 pct.

IV. DISCUSSION

It has been suggested,[8,9] and this is supported by the current experimental evidence (both optical microscopy and

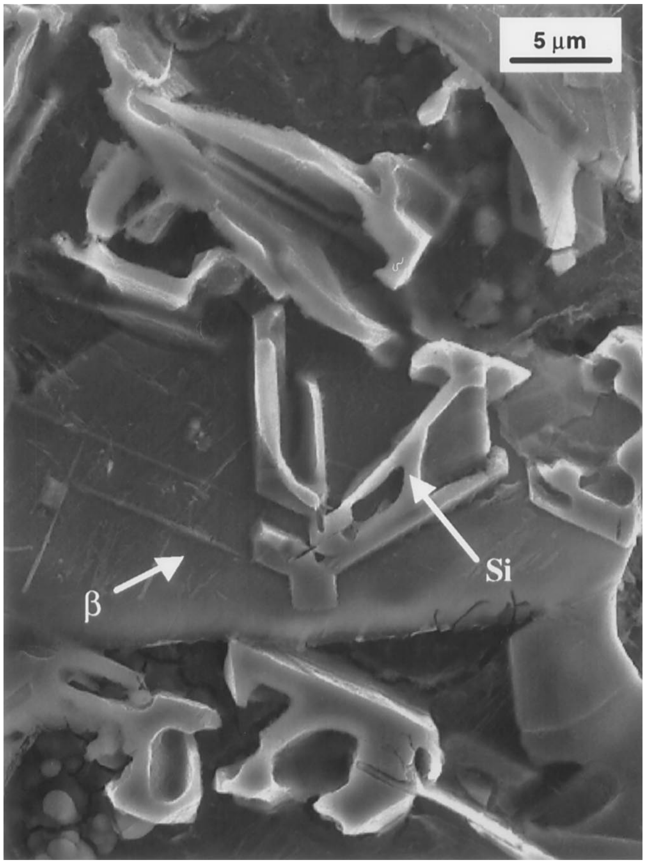

Fig. 3—Secondary electron SEM micrograph showing an embryonic eutectic silicon cell (radiating plates of silicon) that has nucleated and grown on the surface of a β-Al_5FeSi platelet in a deep-etched sample from a B7 segment of an AA309 alloy casting containing 0.7 pct Fe.

SEM), that the unmodified eutectic silicon phase nucleates on the surface of the β platelets (Figures 1 through 3). However, the implications of this observation on the development of porosity do not appear to have been considered previously. The development of shrinkage porosity in hypoeutectic Al-Si–based alloys may arise during the interdendritic feeding stage, when large volume fractions of eutectic silicon are solidifying. Any changes to the microstructural evolution which alter interdendritic permeability during these crucial feeding stages may, therefore, have a significant impact on the formation of porosity.

It can be shown that a feasible orientation relationship exists for the nucleation and growth of silicon on β platelets. This relationship is

$$(210)_{\beta} \parallel (200)_{Si} \cdot [001]_{\beta} \parallel [001]_{Si}$$

where $d_{(210)\beta} = 2.736$ nm and $d_{(200)Si} = 2.715$ nm (a mismatch of 0.77 pct).

For eutectic silicon to nucleate and grow on the β platelets, the latter must pre-exist the former. This is the case for the platelets that form as either a primary β phase or as binary β phase (a component of the Al-βAl_5FeSi binary eutectic). Such platelets are well developed by the time the ternary eutectic silicon begins to grow. However, whether the ternary β platelets of the Al-Si-βAl_5FeSi eutectic can participate in the nucleation of silicon is not as self-evident. Metallographic investigations of both alloy systems (AA309 and its Al-10 pct Si variant) at all iron concentrations show that β platelets of all possible sizes apparently participate in the nucleation of unmodified eutectic silicon. Since platelet size is likely to be a reasonably useful indicator of origin (*i.e.*, larger platelets are more likely to be primary or binary β rather than ternary β, because they had longer to grow), it can be inferred that the ternary β platelets must be the first component of the ternary eutectic to form. The β-Al_5FeSi phase is known to nucleate on aluminium oxide[10] and, since this is common in all aluminum-based melts, the nucleation of β is probably very easy. This assumption is also supported by the absence of any significant undercooling for the β-related inflections on the measured cooling curves. The silicon component of the ternary eutectic may, therefore, nucleate either on the small ternary β phases or on any of the larger binary β platelets already in existence.

Solidification in a simple binary hypoeutectic Al-Si alloy results in two distinct microstructural regimes with differing permeability characteristics. These are the growth of the coherent network of aluminium dendrites and the growth of faceted eutectic silicon cells in the interdendritic spaces. The presence of iron in the hypoeutectic Al-Si alloy system is a complicating factor, with other microstructural regimes becoming possible. The interdendritic permeability and feedability of each regime are likely to be quite different from the others. These regimes are illustrated schematically in Figure 4.

At the critical iron content (Fe_{crit}), the alloy will solidify in two stages (Figure 4(a)): (1) development of the α-aluminum dendritic network, and (2) the formation of the ternary Al-Si-β eutectic in the interdendritic spaces. The aluminum and

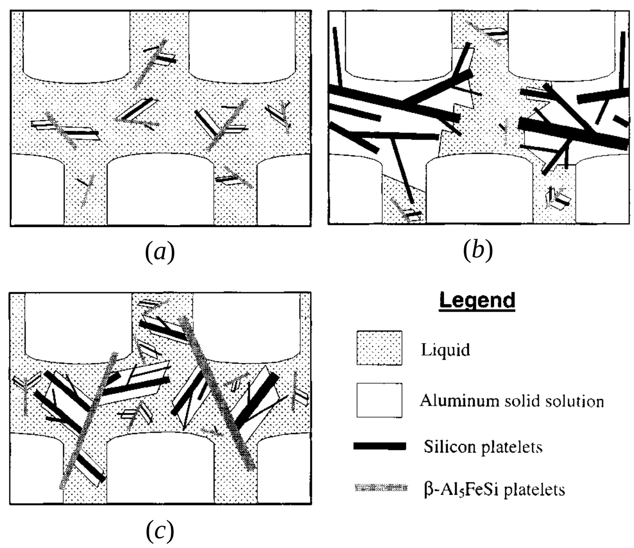

Fig. 4—Schematic representations of the developing microstructure at the point where the ternary Al-Si-βAl_5FeSi eutectic begins to form in an unmodified hypoeutectic Al-Si alloy with iron levels of (*a*) equal to Fe_{crit}, (*b*) below Fe_{crit}, and (*c*) above Fe_{crit}. In each diagram, there are five aluminum dendrite tips and a pool of interdendritic liquid (dotted). The gray needles represent the β-Al_5FeSi platelets (the large ones in (c) are binary β, which forms prior to the ternary eutectic, while the small ones in each diagram, called ternary β, are the first component of the ternary eutectic to form). The mixed white/black striped cells of various sizes are the Al-Si faceted eutectic (the silicon component is black). Note that in (a) the eutectic cells nucleate only on small ternary β platelets. In (b), large eutectic cells (left and right) nucleate independently and prior to the smaller eutectic cells that nucleate on the ternary β platelets. In (c), medium sized eutectic cells nucleate on existing large scale binary β platelets before small scale cells nucleate on the ternary β platelets.

Table I. Five Suggested Types of Microstructural/ Permeability Change in Iron-Containing Hypoeutectic Al-Si Alloys

Type of Microstructural Change	Effect on Microstructural Permeability
α-Al dendrite formation	Grain growth and dendrite arm thickening result in a narrowing of the intergranular and interdendritic spaces.
Growth of Al-β binary eutectic	Formation of binary β platelets within the interdendritic and intergranular spaces, and their subsequent growth and thickening both increase the number of interdendritic channels and reduce the average channel size.
Growth of Al-Si eutectic cells from binary β platelets	The already fragmented and reduced channels become further reduced in size and roughened as the faceted eutectic Si cells grow from multiple nucleation sites along the β platelets.
Growth of Al-Si eutectic cells from non-β substrates	Faceted eutectic cells may grow from several independent sites and gradually fill the interdendritic regions and reduce the permeability.
Growth of Al-Si-β ternary eutectic cells	The β phase forms first in the remaining interdendritic liquid and then the faceted Al-Si cells grow from it. The many small eutectic cells cause further reductions to the interdendritic permeability.

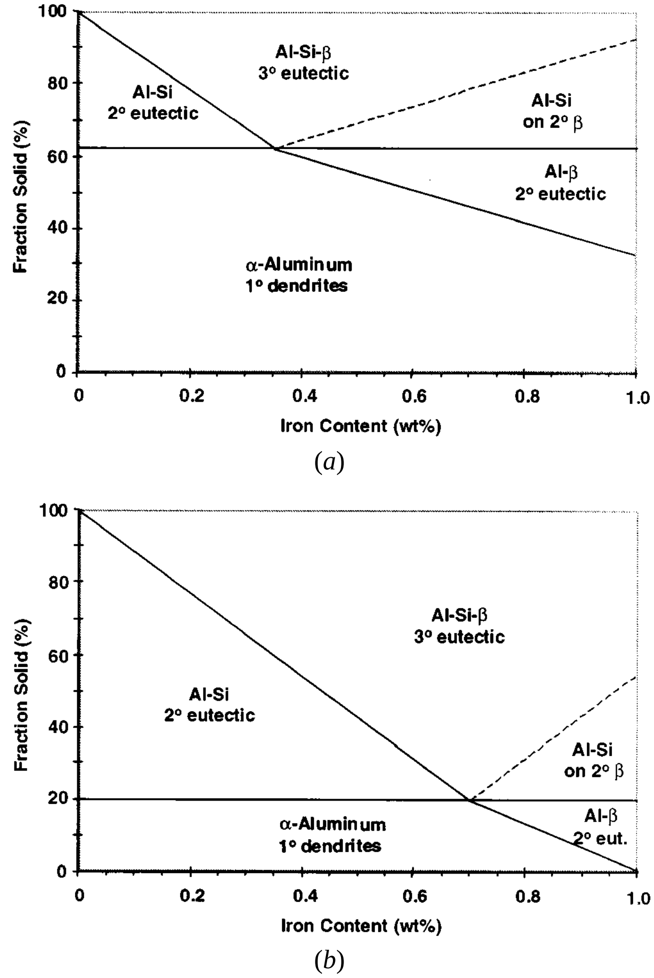

Fig. 5—Graphs showing estimates of the relative proportions of various microstructural types that are predicted to form during solidification at various iron contents in two alloys: (*a*) AA309 alloy and (*b*) Al-10 pct Si alloy. The abbreviations 1°,2°, and 3° stand for primary, binary, and ternary, respectively. A vertical line drawn at any iron content can be used to indicate the sequence of microstructural transformations that might occur during solidification and the approximate fraction solids of formation. The precise positions of the dotted lines between the "A1-Si-β 3°" and the "A1-Si on 2°β" fields are unknown.

silicon components of the ternary eutectic grow on the easier-to-nucleate ternary β platelets. At subcritical iron contents ($<Fe_{crit}$), the alloy solidifies in three stages (Figure 4(b)): (1) development of the α-aluminum dendritic network, (2) the formation of the Al-Si binary eutectic cells that nucleate at non-β sites, and (3) the formation of independently nucleated ternary eutectic cells that nucleate on ternary β platelets. At supercritical iron contents ($>Fe_{crit}$), the alloy solidifies in either three or, possibly, four stages (Figure 4(c)): (1) the development of the α-aluminum dendritic network, (2) the formation of the Al-β binary eutectic, (3) the growth of ternary eutectic cells that nucleate on binary β platelets, and (4) the growth of other independently nucleated ternary eutectic cells. The latter two stages may occur simultaneously. These microstructural changes and their effect on permeability and, therefore, on feeding are described in Table I.

Although the previous sequences are described in terms of the alloy's critical iron content, the relative proportions of each microstructural type formed and the fraction solid at which there is a transition from one microstructural type to another will vary with both the iron and silicon content. Figure 5 provides estimates of the sequence of formation and the approximate proportions of the various microstructural constituents for the two experimental alloys (the small amounts of higher-order Cu and Mg-containing phases are ignored, as they account for less than 5 vol pct).

The large binary β-Al_5FeSi platelets that form in alloys with supercritical iron contents may contribute to the formation of significant regions of interconnected shrinkage porosity through a number of mechanisms, including (1) direct physical obstruction to liquid flow during the interdendritic feeding stage, (2) indirect obstruction to liquid flow by induced changes to the freezing pattern of the eutectic silicon phase, and/or (3) by physically strengthening the dendritic network against collapse and burst feeding.

As the iron content increases above Fe_{crit}, an increasing amount of binary β platelets form in the interdendritic spaces. This creates a rapid multiplication in the number of channels per unit area and a decrease in the average channel size. The permeability decreases according to Eq. [2] and, hence, feedability also decreases. At the ternary eutectic point, the small channels become rapidly narrowed, choked, and roughened as faceted eutectic silicon cells nucleate and grow from the already existing binary β platelets (Figure

4(c)). This results in an increase in the tortuosity and a further decrease in permeability. The proportion of the microstructure that evolves in this deleterious manner increases with iron content (Figure 5). There is, therefore, a corresponding increase in the probability of localized feeding problems occurring with increasing iron content. In such high-iron alloys, major shrinkage-porosity defects are, therefore, more typically found to be located in regions where marginal thermal and feeding conditions exist. In addition, large β platelets that form "bridges" between dendrites may also provide additional strength to the dendritic network. Such strengthening could restrict the later solid feeding mechanisms, and this may explain why massive interconnected porosity defects occur at high iron contents rather than localized surface slumping. Further work is necessary to substantiate this proposition.

The minimum porosity levels observed in the experimental castings at Fe_{crit} in both alloys (*i.e.*, 0.4 pct in AA309 and 0.7 pct in the Al-10 pct Si variant)[4,5] suggest that the permeability of the system is maximized at these compositions. At Fe_{crit}, the dendritic network remains open to a higher fraction solid value than that which occurs at either sub- or supercritical iron contents. Below Fe_{crit}, the Al-Si binary eutectic forms several volume percentage points prior to the start of the ternary eutectic. Above Fe_{crit}, aluminum dendritic growth ceases much earlier and binary Al-βAl$_5$FeSi eutectic growth takes over, up to the point of ternary eutectic formation. As the iron content moves to either side of Fe_{crit}, one or the other of the previous two growth conditions will increase in importance, and, therefore, the permeability of the network is expected to decrease. In addition, the presence of low thermal gradients is likely to encourage random, nondirectional growth of these Al-Si eutectic and Al-β eutectic "cells." Such growth may increase both n and τ values, further decreasing permeability as the iron content diverges to either side of Fe_{crit}.

Not only is the dendritic network permeability likely to be maximized at Fe_{crit}, but the amount of ternary eutectic is also maximized (Figure 5). It may be possible in the early stages of ternary eutectic solidification that the small, embryonic eutectic cells are capable of behaving in a slurry-like manner for a short period prior to becoming a coherent eutectic network (Figure 4(a)). Such interdendritic liquid behavior would optimize feeding.

V. FURTHER CONSIDERATIONS

It is well documented that iron has a deleterious effect on the mechanical properties of Al-Si–based casting alloys,[11,12] due to the presence of the large β-Al$_5$FeSi platelets favored by slow cooling rates (*i.e.*, <5 °C/s).[13] Consequently, various approaches to controlling the formation of the β phase have been developed. These generally encourage the formation of alternative iron-containing intermetallic phases, by either the addition of iron-controlling elements such as Mn, Cr, Co, and Be[12–15] or by the application of thermal treatments to the melt.[10,16,17]

If, as the present theory suggests, the presence of the β platelets arising from the binary Al-βAl$_5$FeSi eutectic are responsible (directly or indirectly) for the development of localized shrinkage defects, then it might be possible to extend the application of these iron-controlling principles for mechanical-property improvement to the control of iron-related porosity defects. Evidence from Iwahori *et al.*[2] has shown that the elements Mn and Be improve the feeding characteristics and reduce shrinkage-porosity formation in an Al-6.8 pct Si-3.2 pct Cu alloy (Japanese code AC2B) that contains detrimentally high levels of iron. Clearly, this could be a useful area for future work.

VI. CONCLUSIONS

In unmodified, nongrain-refined hypoeutectic Al-Si alloys containing approximately 1 pct Cu and 0.5 pct Mg, the β-Al$_5$FeSi platelets (whether formed as components of the binary Al-β or of the ternary Al-Si-β eutectics) have been observed to actively participate in the nucleation of eutectic silicon. The iron and silicon content of the alloy determines at which point during the solidification sequence the β phase appears and, therefore, when it can participate in the silicon nucleation event.

It is, therefore, proposed that, at Fe_{crit} compositions where the maximum possible amount of ternary eutectic forms, the alloy solidifies with the most-open and permeable dendritic network and, possibly, with the most mobile interdendritic feed liquid. As a consequence, feeding is optimized at these compositions and the lowest porosity values exist. At iron contents to either side of Fe_{crit}, there is a smaller proportion of ternary eutectic formation and, hence, porosity formation increases as the situation becomes dominated by the increasing amounts of either the Al-Si or Al-β binary eutectic, both of which reduce permeability. The Al-β is the more detrimental of the two eutectics, with the formation of major shrinkage porosity defects occurring more frequently and more severely as the proportion of the Al-β eutectic increases.

ACKNOWLEDGMENTS

The Cooperative Research Centre for Alloy and Solidification Technology (CAST) was established under and is funded in part by the Australian Government's Cooperative Research Centre Scheme.

REFERENCES

1. M. Claude Mascré: *Fonderie*, 1955, vol. 108, pp. 4330-36.
2. H. Iwahori, H. Takamiya, K. Yonekura, Y. Yamamoto, and M. Nakamura: *Casting*, 1988, vol. 60(9), pp. 590-95.
3. J.E. Eklund: Ph.D. Thesis, Helsinki University of Technology, Helsinki, Finland, 1993.
4. J.A. Taylor, G.B. Schaffer, and D.H. StJohn: *Metall. Mater. Trans. A*, 1999, vol. 30A, pp. 1643-50.
5. J.A. Taylor, G.B. Schaffer, and D.H. StJohn: *Metall. Mater. Trans. A*, 1999, vol. 30A, pp. 1651-55.
6. N. Roy, A.M. Samuel, and F.H. Samuel: *Metall. Mater. Trans. A*, 1996, vol. 27A, pp. 415-29.
7. T.S. Piwonka and M.C. Flemings: *Trans. TMS-AIME*, 1966, vol. 236, pp. 1157-65.
8. M.H. Mulazimoglu, N. Tenekedjiev, B.M. Closset, and J.E. Gruzleski: *Cast Met.* 1993, vol. 6 (1), pp. 16-28.
9. L. Anantha Narayanan, F.H. Samuel, and J.E. Gruzleski: *AFS Trans.*, 1992, vol. 100, pp. 383-91.
10. L. Anantha Narayanan, F.H. Samuel, and J.E. Gruzleski: *Metall. Mater. Trans. A*, 1994, vol. 25A, pp. 1761-73.
11. D. Vorren, J.E. Evensen, and T.B.Pederson: *AFS Trans.*, 1984, vol. 92, pp. 459-66.

12. S. Murali, K.S. Raman, and K.S.S. Murthy: *Cast Met.*, 1994, vol. 6 (4), pp. 189-98.
13. A. Couture: *AFS Int. Cast Met. J.*, 1981, Dec. pp.9-17.
14. G. Gustafsson, T. Thorvaldsson, and G.L. Dunlop: *Metall. Trans. A*, 1986, vol. 17A, pp. 45-52.
15. L. Wang, M. Makhlouf, and D. Apelian: *Int. Mater. Rev.*, 1995, vol. 40(6), pp. 221-38.
16. Y. Awano and Y. Shimizu: *AFS Trans.*, 1990, vol. 98, pp. 889-95.
17. B. Xiufang, Z. Guohua, Z. Sengxu, and M. Jiaji: *Cast Met.*, 1992, vol. 5(1), pp. 39-41.